



Driving-torque self-adjusted triboelectric nanogenerator for effective harvesting of random wind energy[☆]

Yuqi Wang^{a,1}, Xiang Li^{a,1}, Xin Yu^{a,1}, Jianyang Zhu^{a,b}, Ping Shen^c, Zhong Lin Wang^{a,d,*}, Tinghai Cheng^{a,**}

^a Beijing Institute of Nanoenergy and Nanosystems, Chinese Academy of Sciences, Beijing 101400, China

^b Institute of Robotics and Intelligent Systems, Wuhan University of Science and Technology, Wuhan 430081, China

^c State Key Laboratory of Internet of Things for Smart City and Department of Civil and Environmental Engineering, University of Macau, Macao 999078, China

^d School of Materials Science and Engineering, Georgia Institute of Technology, Atlanta, GA 30332-0245, United States

ARTICLE INFO

Keywords:

Triboelectric nanogenerators
Driving-torque self-adjusted
Random wind energy
Effective harvesting

ABSTRACT

Triboelectric nanogenerators (TENGs), as a new energy technology for distributed power, are used widely in the field of the natural environment energy harvesting. Because the natural energy is random and unstable, dynamic matching between TENGs driving-torque and natural environment energy is fundamental for improving the applications of TENGs. Therefore, a driving-torque self-adjusted triboelectric nanogenerator (SA-TENG) for effective harvesting of random wind energy is developed in this paper. When the external wind speed is unstable, the SA-TENG automatically self-adjusted its driving-torque to dynamically match the wind speed and obtain higher output power. Experiments showed that the SA-TENG can adjust its driving-torque in accordance to the wind speed ranging in 5.0–13.2 m/s, and that, the output peak power can reach 7.69 mW. Under the same conditions, in comparison with a normal TENG, the power growth rate and the highest energy conversion efficiency of the SA-TENG were boosted by more than 4.3 and 12.2 times, respectively; values that are also 3.2 and 6.5 times higher, respectively, than those of an electromagnetic generator. Additionally, the SA-TENG can supply power to sensors for monitoring environment, proving its feasibility as a distributed energy source.

1. Introduction

With the continuous improvement of technology, modern society is in the era of big data and intelligent life [1,2]. However, behind the development of science and technology is the massive demand for energy, which has prompted many countries to vigorously research and develop clean and renewable energy [3,4]. To meet the enormous demand for energy by the trillions of sensors distributed worldwide, the effective development of distributed energy is imperative [5,6]. The current mainstream approach to powering distributed sensors is through the power grid or batteries, which impose a high economic burden and substantial negative impact on the natural environment [7,8]. Therefore, it is essential to develop more appropriate technology for

distributed energy.

The triboelectric nanogenerator (TENGs), driven by Maxwell's displacement current, was proposed for the first time by Wang's group in 2012 [1,9]. By coupling triboelectricity and electrostatic induction, mechanical energy can be effectively converted into electrical energy by a TENG [10–14]. Natural environmental energy harvesting mainly involves sources such as wave energy [15–18], vibration energy [19–21], human movement energy [22–25], and wind energy [26]. Among them, wind energy is widely distributed and has large reserves globally; therefore a wind-driven TENGs is highly suitable as a distributed energy source [27–29]. Currently, the performance of a wind-driven TENGs can be improved through its mechanism [30–34], circuitry [18,35], materials [36–39], and on the basis of theory [40–42]. In particular, the

[☆] Prof Zhong Lin Wang, an author on this paper, is the Editor-in-Chief of Nano Energy, but he had no involvement in the peer review process used to assess this work submitted to Nano Energy. This paper was assessed, and the corresponding peer review managed by Professor Chenguo Hu, also an Associate Editor in Nano Energy.

* Corresponding author at: Beijing Institute of Nanoenergy and Nanosystems, Chinese Academy of Sciences, Beijing 101400, China.

** Corresponding author.

E-mail addresses: zhong.wang@mse.gatech.edu (Z.L. Wang), chengtinghai@binn.cas.cn (T. Cheng).

¹ These authors contributed equally to this work.

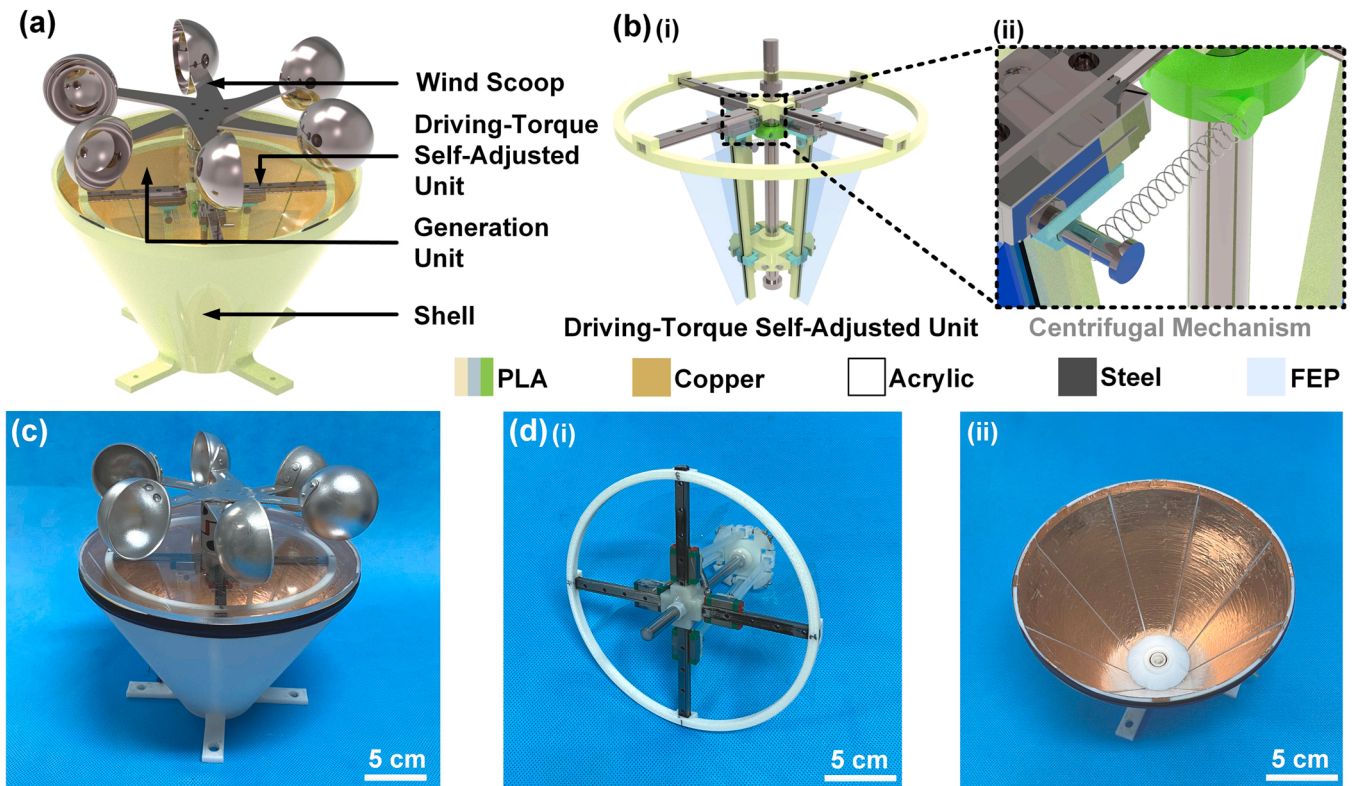


Fig. 1. The driving-torque self-adjusted triboelectric nanogenerator (SA-TENG): (a) schematic showing the overall structure of the SA-TENG, (b) schematic of the driving-torque self-adjusted unit, and (c) and (d) photographs of the SA-TENG, rotor, and stator.

physical machinery has characteristics of robustness and low cost that make it an important area in which to improve wind-driven TENGs performance [43–46]. In the natural environment, wind energy has the characteristics of randomness, instability, and a wide range of wind speed changes [47,48]. Therefore, if TENGs driving-torque could be automatically adjusted to match the external input energy by a mechanical structure, and the approximate error between the actual power and the desired power were reduced continuously, the output power of a

TENG could be increased substantially. The primary parameters affecting TENGs driving-torque are centrifugal force and effective generation area. Therefore, the designed mechanical structure should ideally be able to automatically adjust both the torque and the effective generation area when the wind speed changes.

In this work, a driving-torque self-adjusted (SA-TENG) was developed for the efficient harvesting of random wind energy. The SA-TENG applies an internal driving-torque self-adjusted unit to realize dynamic matching between the effective generation area and the external wind energy. With the change of the external wind speed, the SA-TENG automatically adjusts the parameters that affect the generator driving-torque, e.g., and effective generation area, through varying its own centrifugal force. Thus, the SA-TENG can dynamically adjust its driving-torque to match the wind speed, thereby reducing the difference between the actual power and the expected power. When the external wind speed fluctuates, the driving-torque of the SA-TENG can be automatically adjusted to always match the wind speed. Experiments showed that the power growth rate of the SA-TENG was 3500%, i.e., 4.3 and 3.2 times higher than a normal (N-TENG) and electromagnetic generator (EMG), respectively. Under a random wind environment, the highest energy conversion efficiency of the SA-TENG was boosted by more than 12.2 and 6.5 times in comparison with that of the N-TENG and the EMG, respectively. Application experiments proved that under the same conditions, the charging capacity of the SA-TENG was 2.3 and 18.7 times higher than that of the N-TENG and the EMG, respectively. Additionally, the SA-TENG is able to power the sensors used to monitor the environmental changes, highlighting the potential of the SA-TENG as a distributed energy source. The findings of this research represent important guidance regarding the efficient harvesting of random wind energy using TENGs.

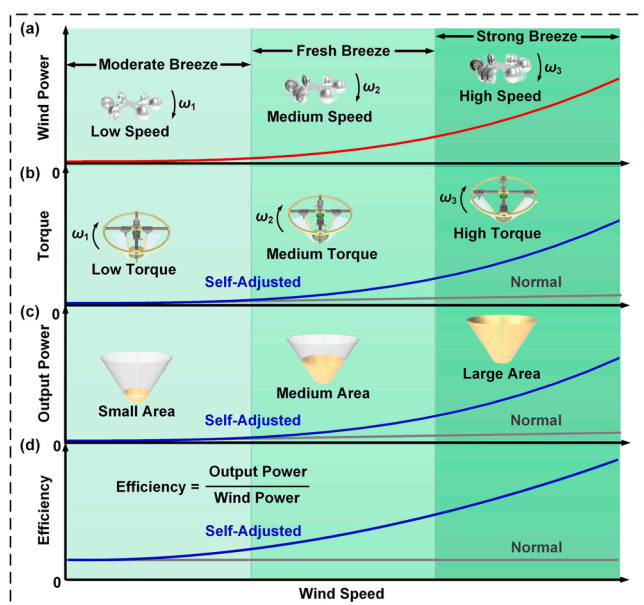


Fig. 2. Working principles of the SA-TENG: (a)–(d) relationships between wind speed and wind energy, torque, output power and efficiency.

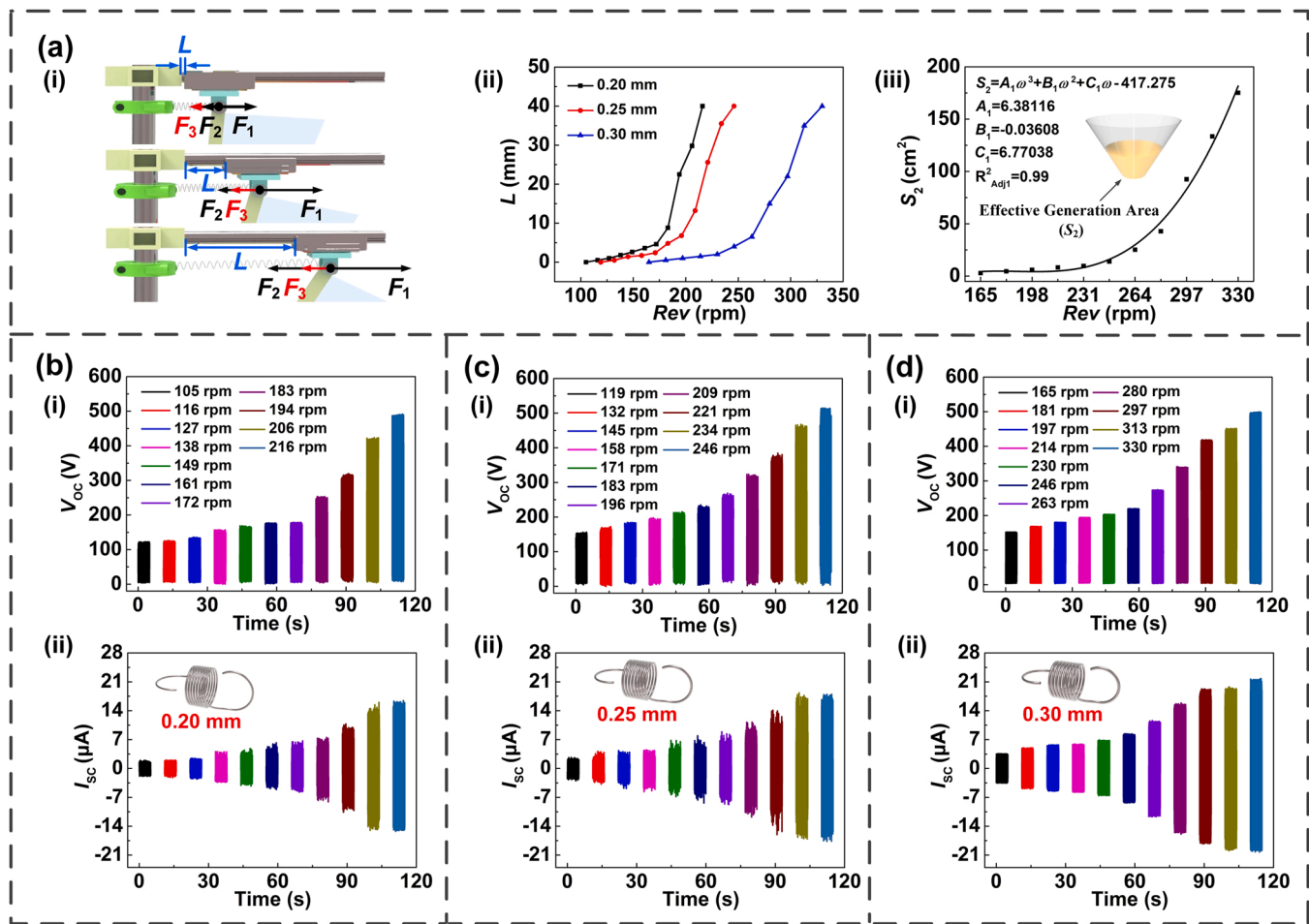


Fig. 3. Output performance of the SA-TENG with spring wires of different diameters: (a) 0.20 mm, (b) 0.25 mm, and (c) 0.30 mm.

2. Results and discussion

2.1. Structure design

N-TENG driving-torque will not change with variation of external input power; therefore, the output power increases slowly with the increase of the input power after excitation. To enable TENG driving-torque to be changed adaptively with the variation of the external input power, this work proposed the SA-TENG. The basic structure of the SA-TENG, displayed in Fig. 1a, consists of the wind scoop, driving-torque self-adjusted unit Fig. 1b(i), generation unit, and shell. In particular, the driving-torque self-adjusted unit consists of four centrifugal mechanisms (Fig. 1b(ii)), and the reason why the SA-TENG can achieve self-adjustment of driving-torque is based on the cooperative operation of these centrifugal mechanisms. A photograph of the as-fabricated SA-TENG device is shown in Fig. 1c, and photographs of the fabricated driving-torque self-adjusted unit and generation unit are shown in Fig. 1d(i) and d(ii), respectively.

2.2. Mechanism of the driving-torque self-adjusted unit

The driving-torque self-adjusted unit is a modern energy-adjusting mechanism that regulates the torque or generation area. The working principles of the driving-torque self-adjusted unit are shown in Fig. 2. For the normal generator, most design parameters (e.g., centrifugal force and effective generation area) that affect the driving-torque are fixed. Therefore, when the torque and effective generation area cannot match the wind speed well, the output power will be low. The driving-

torque self-adjusted unit introduced in the SA-TENG can adjust the torque and generation area such that the driving-torque of the generator can be varied dynamically with wind speed. Wind scoops harvest the random wind energy of the environment directly, and the SA-TENG can automatically adjust to typical environmental conditions of a moderate breeze, fresh breeze, and strong breeze (Fig. 2a). The calculation of wind power is shown in Eq. (S1). To achieve dynamic matching between generation area and external input energy, the generation area of SA-TENG should also increase exponentially with wind speed. Therefore, this article designed the FEP film into a trapezoid shape. The torque and generation area of the SA-TENG will automatically adjust to the wind speed, but those of the normal generator will not (Fig. 2b and c). Therefore, SA-TENG is more efficient than normal generator. In this study, 3D simulations using COMSOL were employed to elucidate the working principles of the SA-TENG to demonstrate the feasibility of the approach (Fig. S1).

2.3. Output performance

The essential factor of the SA-TENG is self-adjustment of its output performance to the external input energy. To measure the output performance of the SA-TENG, a method was adopted in which the stepper motors offered different input rotation speeds. Fig. 3a(i) illustrates the forces acting when the SA-TENG is running, where F_1 is the resultant force of the tension spring force (F_2) and the static friction force (F_3). Because F_3 is fixed, the value of F_1 is affected solely by F_2 . The range of rotation speed (n) for each of the three tension springs (diameter: 0.20, 0.25, and 0.30 mm) is 105–216, 120–246, and 165–330 rpm,

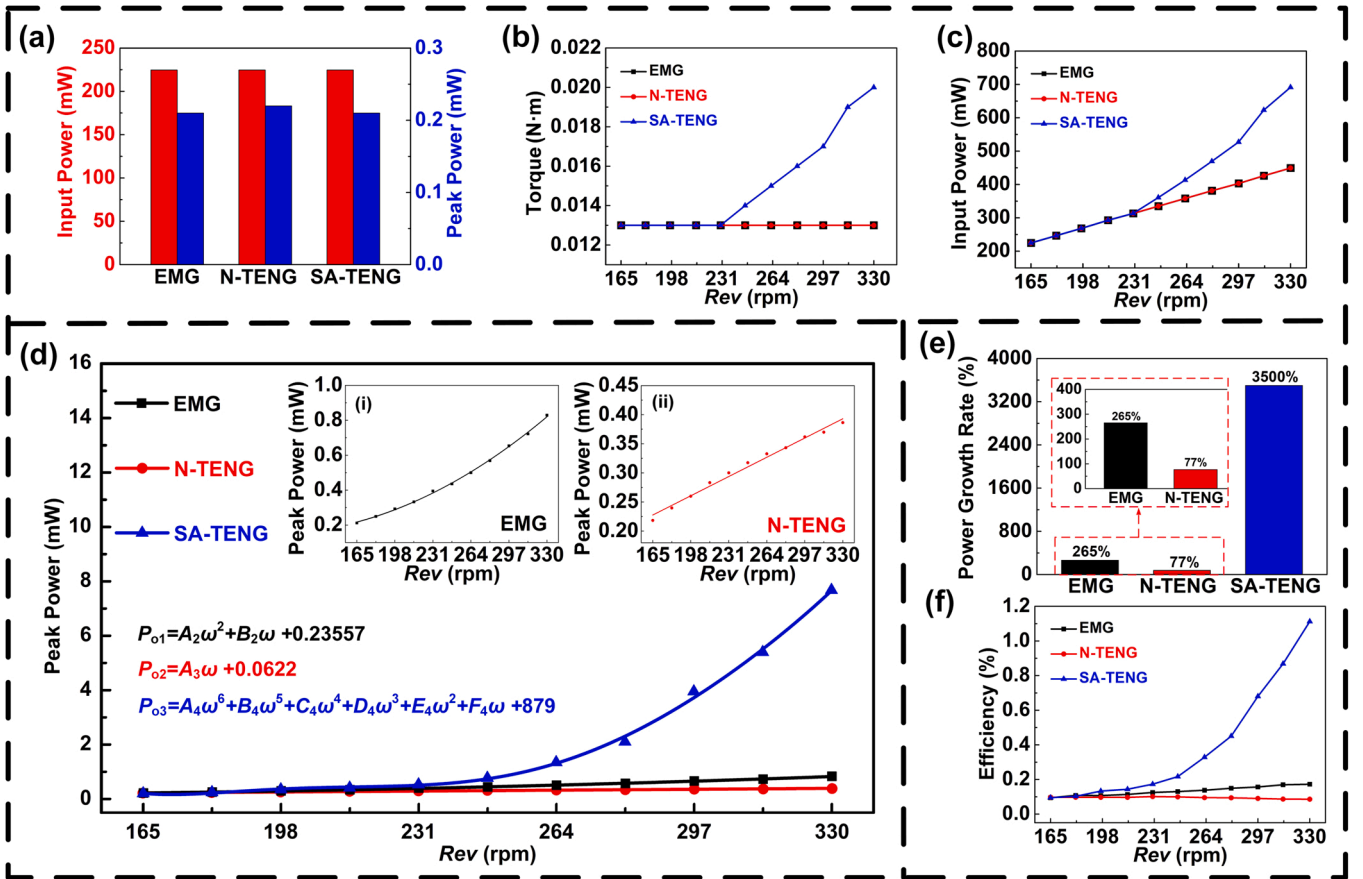


Fig. 4. Comparison of performance of the three different generators: (a) input power and output power when n is 165 rpm, and (b) torque, (c) input power, (d) output power, (e) power growth rate, and (f) efficiency when n is varied.

respectively (Fig. 3a(ii)). In particular, the inflection point of the curve of each of the tension springs is approximately the sixth, which is because F_1 is approximately equal to F_2 . The relationship between displacement distance of slider (L) and n is shown by Eqs. (S2)–(S6). Fig. S2 shows the torque produced by the different tension springs when they rotate. The torque range of each of the three tension springs (diameter: 0.20, 0.25, and 0.30 mm) is 0.008–0.015, 0.01–0.017, and 0.013–0.02 N·m, respectively. To allow driving-torque self-adjusted by the SA-TENG, a trapezoidal section of FEP film is included, and the relationship between effective generation area (S_2) and rotating speed is shown in Fig. 3a(iii). The output performance related to the different tension springs is illustrated in Figs. 3b–d and S3). In particular, as the rotational speed increases, the output open-circuit voltage and the short-circuit current both show a trend of growth. Because the SA-TENG is easily driven, a smaller wire diameter will lower the upper limit of SA-TENG regulation, this study opted to use a wire tension spring with a diameter of 0.30 mm to allow the SA-TENG to adjust to the typical range of wind speeds found in the natural environment. Moreover, when the diameter of the wire tension spring is 0.30 mm, the output performance of the SA-TENG is better.

2.4. Performance comparison

To study the driving-torque of different generators for random wind energy harvesting, two additional generators were considered: an N-TENG (Fig. S4a) and an EMG (Fig. S4b). The self-adjusted n range of the SA-TENG is 165–330 rpm; therefore, to more clearly compare the capability of the three types of generators to harvest random wind energy, the input power (P_i) and output peak power of each of the three generators at 165 rpm were set to be almost the same (Fig. 4a). The

output performance of EMG is adjusted by changing the parameters of magnets and coils, and the output performance of N-TENG is adjusted by changing the generation area. The calculation of P_i is shown in Eq. (S7). After n was increased from 165 to 330 rpm, the torque (T) of each of the three generators was measured (Fig. 4b). When the rotation speed is lower than 231 rpm, the centrifugal mechanism does not work, so the torque does not change. However, SA-TENG can still rely on the characteristic of FEP film expanding to the outer shell by centrifugal force, to realize the dynamic matching between the generation area and the external input energy. The relationship between P_i and n is shown in Fig. 4c, the average efficiency is shown in Fig. S5.

To accurately compare the adjustment capabilities of the three generators when the external input rotation speed changes, the output power of the three types of the generator was measured (Fig. 4d), the impedance matching data of the three generators are shown in Fig. S6, the output peak power dynamic curves of SA-TENG under different torque conditions are shown in Fig. S7. Output peak power (P_{o1}) of the EMG was derived using Eq. (1):

$$P_{o1} = \frac{(nBS_3\omega)^2}{R}, \quad (1)$$

where B is magnetic field intensity, S_3 is the area of the coil section, and R is the system resistance. The output peak power (P_{o2}) of the N-TENG and output peak power (P_{o3}) of the SA-TENG are influenced by the contact area between the FEP film and the copper. Both P_{o2} and P_{o3} can be obtained using Eq. (2); here, P_{o3} is taken as an example:

$$P_{o3} = \frac{S_2^2 \sigma d \sigma}{C_1 dt}, \quad (2)$$

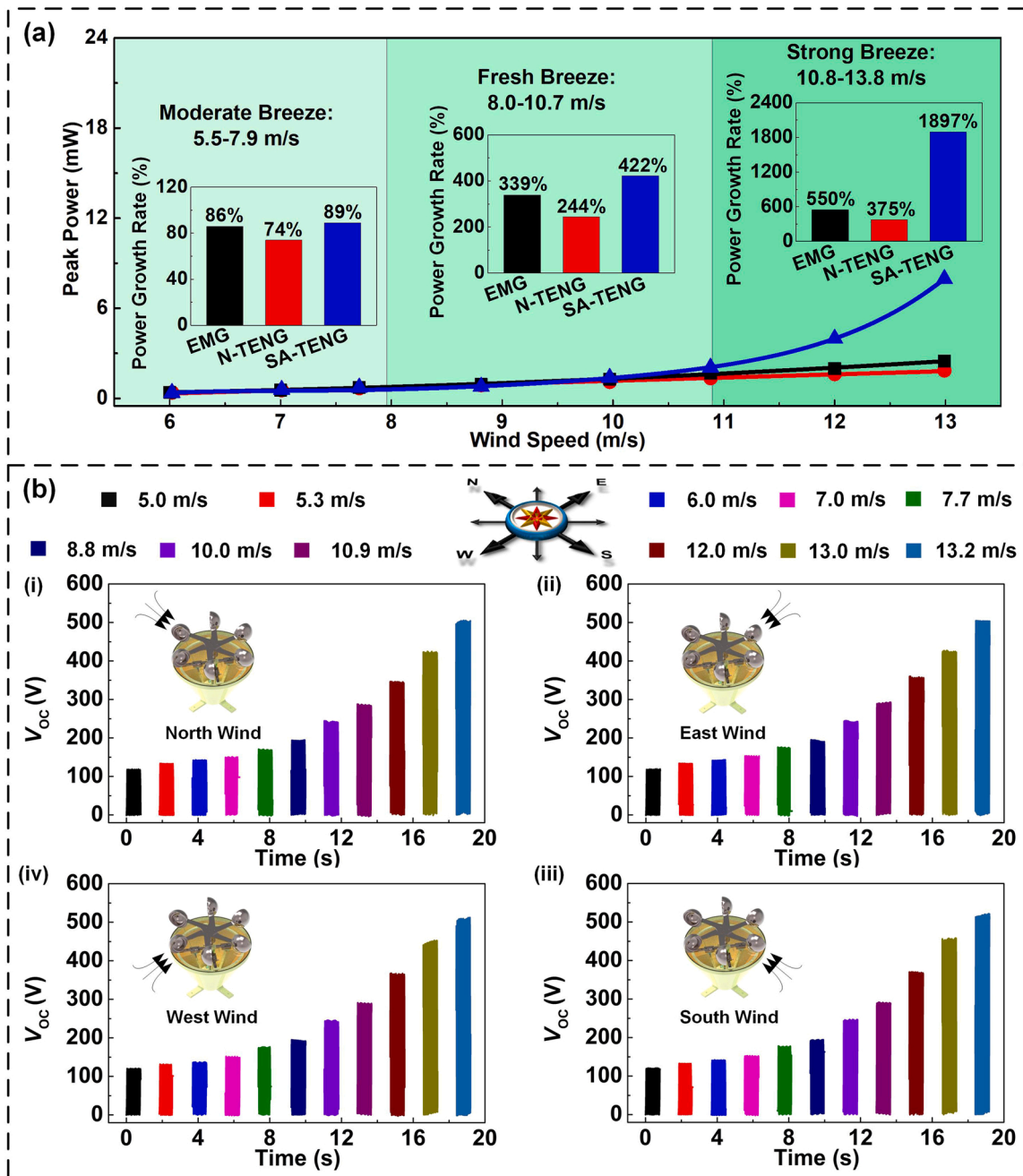


Fig. 5. Experimental measurements under conditions of a simulated natural wind environment: (a) output peak power of the three types of the generator at different wind speeds, and open-circuit voltage for (b) (i) north, (ii) east, (iii) west, and (iv) south wind.

where σ is charge density and C_1 is system capacitance. Therefore, P_{O3} grows faster than either P_{O1} or P_{O2} . The variation of P_{O1} and P_{O2} is shown enlarged in Fig. 4d(i) and d(ii), respectively. Among them, for the specific values of $A_2, A_3, A_4, B_2, B_4, C_4, D_4, E_4, F_4$, please refer to the Fig. S8 in the Supporting information. Further details are provided in Supporting Movie S1. The power growth rates of the EMG (R_{i1}), the N-TENG (R_{i2}), and the SA-TENG (R_{i3}) are shown in Fig. 4e. The power growth rates (R_i) are defined as follows:

$$R_i = \frac{P_{O-\max} - P_{O-\min}}{P_{O-\min}} \times 100\% \quad (3)$$

Supplementary material related to this article can be found online at [doi:10.1016/j.nanoen.2022.107389](https://doi.org/10.1016/j.nanoen.2022.107389).

Supplementary material related to this article can be found online at [doi:10.1016/j.nanoen.2022.107389](https://doi.org/10.1016/j.nanoen.2022.107389).

To prove the capability of the SA-TENG to harvest wind energy, the SA-TENG was assessed in relation to the simulated moderate breeze, fresh breeze, and the strong breeze environments, as shown in Fig. 5. The peak power in a simulated natural wind environment was also investigated (Fig. 5a), the average power is shown in Fig. S9. Additionally, the power growth rates are shown in the illustrations. Here, R_{i1} , R_{i2} , and R_{i3} are 550%, 375%, and 1897%, respectively. The power growth rates calculated when the generator is driven by wind power are smaller than those when the generator is driven by a stepper motor. Because the driving-torque of each of the three types of a generator is different at the same wind speed, the n of the generators is different. When the wind comes from the four directions of north, east, south, and west, the open-circuit voltage (Fig. 5b) is almost the same. This proves the stability of the SA-TENG. The wind speed range was 5.0–13.2 m/s in this experiment.

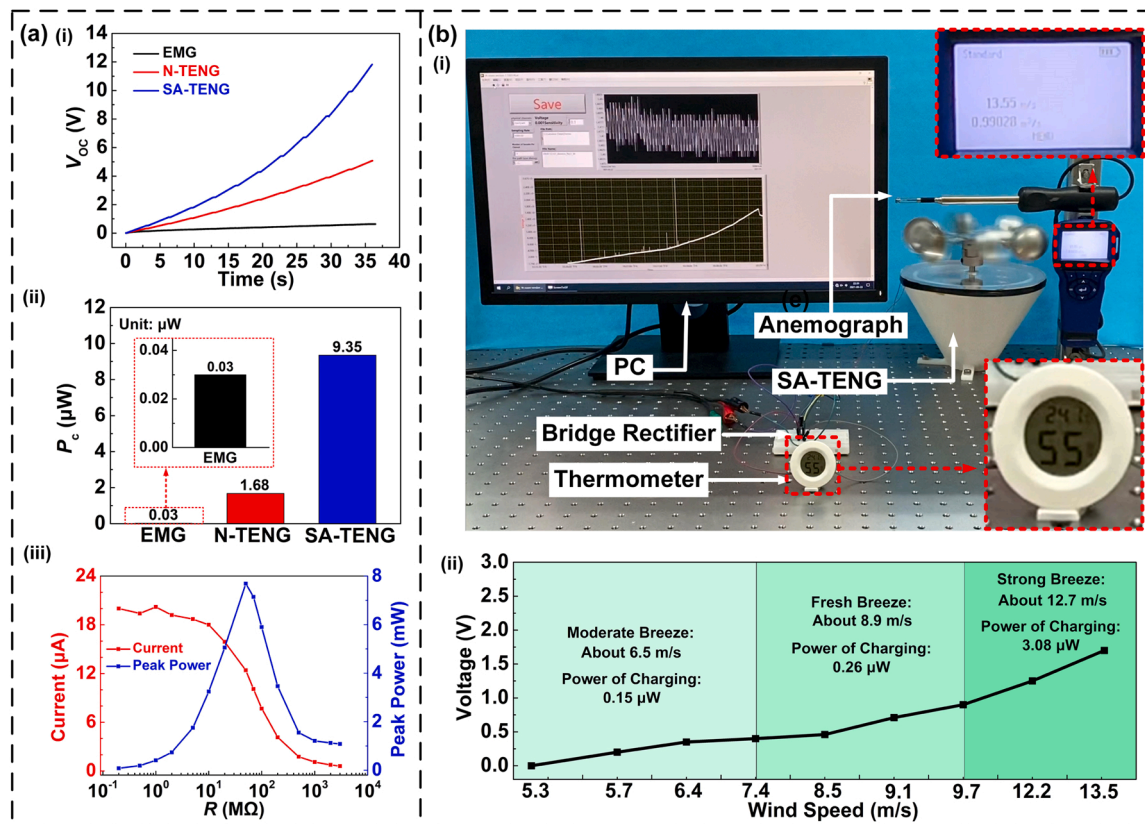


Fig. 6. Comparison of application capability of different generators. (a) (i) Commercial 4.7 μF capacitor charged from 0 to 36 s, (ii) P_c of the different generators, and (iii) peak power of the SA-TENG for different rotational speeds. (b) (i) Experimental platform in the environment of a simulated wind, and (ii) the relationship between wind speed and capacitor voltage.

2.5. Demonstrations

To prove the application capability of the SA-TENG, the charging capacity of the EMG, N-TENG, and SA-TENG was compared. In 36 s, a 0.47 μF capacitor was charged to 0.64, 5.07, and 11.97 V by the EMG, N-TENG, and SA-TENG, respectively (Fig. 6a(i)). The power of charging (P_c) of the EMG, N-TENG, and SA-TENG was 0.03, 1.68, and 9.35 μW , respectively, for a 4.7 μF capacitor (Fig. 6a(ii)). The load peak power of the SA-TENG is shown in Fig. 6a(iii). In addition, the durability experiment of SA-TENG is shown in Fig. S10. The maximum peak power was 7.69 mW. Additionally, the powering of a commercial thermometer is demonstrated in Fig. 6b(i). Further details are shown in Supporting Movie S3, which considers the wind environments of a moderate breeze, fresh breeze, and strong breeze. The corresponding charged voltages of capacitors at different wind speeds are shown in Fig. 6b(ii).

Supplementary material related to this article can be found online at [doi:10.1016/j.nanoen.2022.107389](https://doi.org/10.1016/j.nanoen.2022.107389).

3. Conclusions

In this study, a SA-TENG was developed to address the problem of mismatch between generator driving-torque and input energy. When the wind speed fluctuates, the SA-TENG can change the torque and effective generation area through variation of the centrifugal force, thereby realizing dynamic matching between its driving-torque and the external input wind energy, and improving output performance. Experiments showed that when the external input rotation speed fluctuated, the power growth rate of the SA-TENG was 3500%, i.e., 4.3 and 3.2 times higher than that of the N-TENG and the EMG, respectively. The charging capacity of the SA-TENG was boosted by more than 2.3 and 18.7 times in comparison with that of the N-TENG and the EMG. Within the self-

adjusting range of the SA-TENG, the energy conversion efficiency of the SA-TENG was higher than that of the other two generators. In the simulated wind environments, the SA-TENG was shown able to harvest wind energy normally from different directions. Demonstration experiments showed that the SA-TENG can successfully power temperature and humidity sensors, proving its feasibility as a distributed energy source. The SA-TENG has bright application prospects in terms of effective harvesting of random wind energy, and the findings of this study could represent an essential reference for TENG design.

4. Experimental section

4.1. Fabrication method

The SA-TENG has dimensions of 200 mm (length) \times 200 mm (width) \times 210 mm (height). The shells of the SA-TENG are fabricated by 3D printing and laser cutting, the printed material being polylactic acid (PLA), and the laser cutting material being acrylic. The driving-torque self-adjusted unit of the SA-TENG is machined using a lathe. The fluorinated ethylene propylene (FEP) film has a thickness of 100 μm and width of 50 mm. Eight copper electrodes with a thickness of 0.065 mm are evenly distributed on the inner wall of the stator in the generation unit. Other information is given as Supporting information.

4.2. Electrical measurement

The rotation is generated by a stepper motor (J-5718HBS401, Yisheng, China) and measured by the torque sensor (DR-2112-R, Lorenz Messtechnik, Germany), and the signal of SA-TENG was harvested by a programmable electrometer (6514, Keithley, USA) and a data acquisition card (USB-6218, National Instruments, USA). The signal is

transmitted to the computer and recorded by LabVIEW.

CRedit authorship contribution statement

Yuqi Wang: Conceptualization, Investigation, **Xiang Li:** Investigation, Writing - original draft, Validation, **Xin Yu:** Investigation, Validation, **Jiayang Zhu:** Investigation, Editing, **Ping Shen:** Validation, **Zhong Lin Wang:** Conceptualization, Resources, Writing – review & editing, Supervision, **Tinghai Cheng:** Conceptualization, Resources, Writing – review & editing, Supervision.

Declaration of Competing Interest

The authors declare that they have no known competing financial interests or personal relationships that could have appeared to influence the work reported in this paper.

Acknowledgments

The authors are grateful for the support from the Beijing Natural Science Foundation (No. 3222023), the Open Research Project Programme of the State Key Laboratory of Internet of Things for Smart City (University of Macau) (No. SKL-IoTSC(UM)-2021-2023/ORPF/A17/2022), the National Key R & D Project from the Minister of Science and Technology (Nos. 2021YFA1201601 and 2021YFA1201604).

Appendix A. Supporting information

Supplementary data associated with this article can be found in the online version at [doi:10.1016/j.nanoen.2022.107389](https://doi.org/10.1016/j.nanoen.2022.107389).

References

- [1] F.-R. Fan, Z.-Q. Tian, Z.L. Wang, Flexible triboelectric generator, *Nano Energy* 1 (2012) 328–334.
- [2] Z.L. Wang, J.H. Song, Piezoelectric nanogenerators based on zinc oxide nanowire arrays, *Science* 312 (2006) 242–246.
- [3] Z.L. Wang, Triboelectric nanogenerators as new energy technology for self-powered systems and as active mechanical and chemical sensors, *ACS Nano* 7 (2013) 9544–9557.
- [4] Z. Yang, Y.Y. Yang, F. Liu, Z.Z. Wang, Y.B. Li, J.H. Qiu, X. Xiao, Z.W. Li, Y.J. Lu, L. H. Ji, Z.L. Wang, J. Cheng, Power backpack for energy harvesting and reduced load impact, *ACS Nano* 15 (2021) 2611–2623.
- [5] S. Yong, J.Y. Wang, L.J. Yang, H.Q. Wang, H. Luo, R.J. Liao, Z.L. Wang, Auto-switching self-powered system for efficient broad-band wind energy harvesting based on dual-rotation shaft triboelectric nanogenerator, *Adv. Energy Mater.* 11 (2021), 2101194.
- [6] L. Atzori, A. Iera, G. Morabito, The internet of things: a survey, *Comput. Netw.* 54 (2010) 2787.
- [7] J.H. Nord, A. Koohang, J. Paliszkiwicz, The internet of things: review and theoretical framework, *Expert Syst. Appl.* 133 (2019) 97.
- [8] Z.Z. Wang, Y.X. Shi, F. Liu, H. Wang, X. Liu, R.T. Sun, Y.J. Lu, L.H. Ji, Z.L. Wang, J. Cheng, Distributed mobile ultraviolet light sources driven by ambient mechanical stimuli, *Nano Energy* 74 (2020), 104910.
- [9] Z.L. Wang, On Maxwell's displacement current for energy and sensors: the origin of nanogenerators, *Mater. Today* 20 (2017) 74–82.
- [10] J.W. Zhong, Q.Z. Zhong, F.-R. Fan, Y. Zhang, S.H. Wang, B. Hu, Z.L. Wang, J. Zhou, Finger typing driven triboelectric nanogenerator and its use for instantaneously lighting up LEDs, *Nano Energy* 2 (2013) 491–497.
- [11] Q. Tang, M.-H. Yeh, G.L. Liu, S.M. Li, J. Chen, Y. Bai, L. Feng, M.H. Lai, K.-C. Ho, H. Y. Guo, C.G. Hu, Whirligig-inspired triboelectric nanogenerator with ultrahigh specific output as reliable portable instant power supply for personal health monitoring devices, *Nano Energy* 47 (2018) 74–80.
- [12] C. Xu, Y.L. Zi, A.C. Wang, H.Y. Zou, Y.J. Dai, X. He, P.H. Wang, Y.C. Wang, P. Z. Feng, D.W. Li, Z.L. Wang, On the electron-transfer mechanism in the contact-electrification effect, *Adv. Mater.* 30 (2018), 1706790.
- [13] Z.L. Wang, T. Jiang, L. Xu, Toward the blue energy dream by triboelectric nanogenerator networks, *Nano Energy* 39 (2017) 9–23.
- [14] J. Cheng, W.B. Ding, Y.L. Zi, Y.J. Lu, L.H. Ji, F. Liu, C.S. Wu, Z.L. Wang, Triboelectric microplasma powered by mechanical stimuli, *Nat. Commun.* 9 (2018) 3733.
- [15] T.C. Zhao, M.Y. Xu, X. Xiao, Y. Ma, Z. Li, Z.L. Wang, Recent progress in blue energy harvesting for powering distributed sensors in ocean, *Nano Energy* 88 (2021), 106199.
- [16] Z.L. Wang, Catch wave power in floating nets, *Nature* 542 (2017) 159–160.
- [17] J. Scruggs, P. Jacob, Harvesting ocean wave energy, *Science* 323 (2009) 1176–1178.
- [18] J.L. Wang, X. Yu, D. Zhao, Y. Yu, Q. Gao, T.H. Cheng, Z.L. Wang, Enhancing output performance of triboelectric nanogenerator via charge clamping, *Adv. Energy Mater.* 11 (2021), 2101356.
- [19] S.X. Li, D. Liu, Z.H. Zhao, L.L. Zhou, X. Yin, X.Y. Li, Y.K. Gao, C.G. Zhang, Q. Zhang, J. Wang, Z.L. Wang, A fully self-powered vibration monitoring system driven by dual-mode triboelectric nanogenerators, *ACS Nano* 14 (2020) 2475–2482.
- [20] A.F. Yu, P. Jiang, Z.L. Wang, Nanogenerator as self-powered vibration sensor, *Nano Energy* 1 (2012) 418–423.
- [21] J. Chen, G. Zhu, W.Q. Yang, Q.S. Jing, P. Bai, Y. Yang, T.-C. Hou, Z.L. Wang, Harmonic-resonator-based triboelectric nanogenerator as a sustainable power source and a self-powered active vibration sensor, *Adv. Mater.* 25 (2013) 6094–6099.
- [22] Q.H. Xu, Y.S. Fang, Q.S. Jing, N. Hu, K. Lin, Y.F. Pan, L. Xu, H.Q. Gao, M. Yuan, L. Chu, Y.W. Ma, Y.N. Xie, J. Chen, L.H. Wang, A portable triboelectric spirometer for wireless pulmonary function monitoring, *Biosens. Bioelectron.* 187 (2021), 113329.
- [23] L. Liu, Q.F. Shi, C.K. Lee, A hybridized electromagnetic-triboelectric nanogenerator designed for scavenging biomechanical energy in human balance control, *Nano Res.* 14 (2021) 4227–4235.
- [24] Y. Yang, H.L. Zhang, Y.S. Zhou, Q.S. Jing, Y.J. Su, J. Yang, J. Chen, C.G. Hu, Z. L. Wang, Human skin based triboelectric nanogenerators for harvesting biomechanical energy and as self powered active tactile sensor system, *ACS Nano* 7 (2013) 9213–9222.
- [25] W.Q. Yang, J. Chen, G. Zhu, P. Bai, Y.J. Su, Q.S. Jing, X. Cao, Z.L. Wang, Harvesting energy from the natural vibration of human walking, *ACS Nano* 7 (2013) 11317–11324.
- [26] H. Wang, M.Y. Zhang, Z. Yang, Z.Z. Wang, X. Liu, Y.J. Lu, L.H. Ji, Z.L. Wang, J. Cheng, Energy from greenhouse plastic films, *Nano Energy* 89 (2021), 106328.
- [27] Z.L. Wang, Triboelectric nanogenerators as new energy technology and self-powered sensors - principles, problems and perspectives, *Faraday Discuss.* 176 (2014) 447–458.
- [28] Z.L. Wang, Entropy theory of distributed energy for internet of things, *Nano Energy* 58 (2019) 669–672.
- [29] Z.L. Wang, Triboelectric nanogenerator (TENG)—sparking an energy and sensor revolution, *Adv. Energy Mater.* 10 (2020), 2000137.
- [30] Q. Gao, Y.K. Li, Z.J. Xie, W.X. Yang, Z. Wang, M.F. Yin, X.H. Lu, T.H. Cheng, Z. L. Wang, Robust triboelectric nanogenerator with ratchet-like wheel-based design for harvesting of environmental energy, *Adv. Mater. Technol.* 5 (2019), 1900801.
- [31] T.H. Cheng, Y.K. Li, Y.-C. Wang, Q. Gao, T. Ma, Z.L. Wang, Triboelectric nanogenerator by integrating a cam and a movable frame for ambient mechanical energy harvesting, *Nano Energy* 60 (2019) 137–143.
- [32] X.M. Fan, J. He, J.L. Mu, J.C. Qian, N. Zhang, C.J. Yang, X.J. Hou, W.P. Geng, X. D. Wang, X.J. Chou, Triboelectric-electromagnetic hybrid nanogenerator driven by wind for self-powered wireless transmission in Internet of things and self-powered wind speed sensor, *Nano Energy* 68 (2020), 104319.
- [33] K.D. Pham, D. Bhatia, N.D. Huynh, H. Kim, J.M. Baik, Z.-H. Lin, D. Choi, Automatically switchable mechanical frequency regulator for continuous mechanical energy harvesting via a triboelectric nanogenerator, *Nano Energy* 89 (2021), 106350.
- [34] S.K. Fu, W.C. He, Q. Tang, Z. Wang, W.L. Liu, Q.Y. Li, C.Y. Shan, L. Long, C.G. Hu, H. Liu, An ultrarobust and high-performance rotational hydrodynamic triboelectric nanogenerator enabled by automatic mode switching and charge excitation, *Adv. Mater.* 34 (2022), 2105882.
- [35] Q.H. Xu, Y.T. Lu, S.Y. Zhao, N. Hu, Y.W. Jiang, H. Li, Y. Wang, H.Q. Gao, Y. Li, M. Yuan, L. Chu, J.H. Li, Y.N. Xie, A wind vector detecting system based on triboelectric and photoelectric sensors for simultaneously monitoring wind speed and direction, *Nano Energy* 89 (2021), 106382.
- [36] Y. Yang, G. Zhu, H.L. Zhang, J. Chen, X.D. Zhong, Z.-H. Lin, Y.J. Su, P. Bai, X. N. Wen, Z.L. Wang, Triboelectric nanogenerator for harvesting wind energy and as self-powered wind vector sensor system, *ACS Nano* 7 (2013) 9461–9468.
- [37] J. Bae, J. Lee, S.M. Kim, J. Ha, B.S. Lee, Y.J. Park, C. Choong, J.B. Kim, Z.L. Wang, H.Y. Kim, J.J. Park, U.I. Chung, Flutter-driven triboelectrification for harvesting wind energy, *Nat. Commun.* 5 (2014) 4929.
- [38] C.Y. Ye, K. Dong, J. An, J. Yi, X. Peng, C. Ning, Z.L. Wang, A triboelectric–electromagnetic hybrid nanogenerator with broadband working range for wind energy harvesting and a self-powered wind speed sensor, *ACS Energy Lett.* 6 (2021) 1443–1452.
- [39] Z.W. Ren, Z.M. Wang, Z.R. Liu, L.F. Wang, H.Y. Guo, L.L. Li, S.T. Li, X.Y. Chen, W. Tang, Z.L. Wang, Energy harvesting from breeze wind (0.7–6 m/s) using ultra-stretchable triboelectric nanogenerator, *Adv. Energy Mater.* 10 (2020), 2001770.
- [40] Y. Bai, L. Xu, S.Q. Lin, J.J. Luo, H.F. Qin, K. Han, Z.L. Wang, Charge pumping strategy for rotation and sliding type triboelectric nanogenerators, *Adv. Energy Mater.* 10 (2020), 2000605.
- [41] L. Cheng, Q. Xu, Y.B. Zheng, X.F. Jia, Y. Qin, A self-improving triboelectric nanogenerator with improved charge density and increased charge accumulation speed, *Nat. Commun.* 9 (2018) 3773.
- [42] Q.Y. Li, W.L. Liu, H.M. Yang, W.C. He, L. Long, M.B. Wu, X.M. Zhang, Y. Xi, C. G. Hu, Z.L. Wang, Ultra-stability high-voltage triboelectric nanogenerator designed by ternary dielectric triboelectrification with partial soft-contact and non-contact mode, *Nano Energy* 90 (2021), 106585.
- [43] Y.N. Xie, S.H. Wang, L. Lin, Q.S. Jing, Z.-H. Lin, S.M. Niu, Z.Y. Wu, Z.L. Wang, Rotary triboelectric nanogenerator based on a hybridized mechanism for harvesting wind energy, *ACS Nano* 7 (2013) 7119–7125.

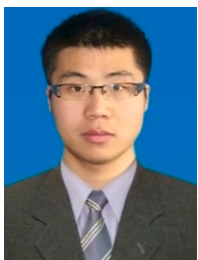
- [44] Z.M. Lin, B.B. Zhang, H.Y. Guo, Z.Y. Wu, H.Y. Zou, J. Yang, Z.L. Wang, Super-robust and frequency-multiplied triboelectric nanogenerator for efficient harvesting water and wind energy, *Nano Energy* 64 (2019), 103908.
- [45] J. Hu, X.J. Pu, H.M. Yang, Q.X. Zeng, Q. Tang, D.Z. Zhang, C.G. Hu, Y. Xi, A flutter-effect-based triboelectric nanogenerator for breeze energy collection from arbitrary directions and self-powered wind speed sensor, *Nano Res.* 12 (2019) 3018–3023.
- [46] J. Chen, H.Y. Guo, C.G. Hu, Z.L. Wang, Robust triboelectric nanogenerator achieved by centrifugal force induced automatic working mode transition, *Adv. Energy Mater.* 10 (2020), 2000886.
- [47] X. Li, Y.Y. Cao, X. Yu, Y.H. Xu, Y.F. Yang, S.M. Liu, T.H. Cheng, Z.L. Wang, Breeze-driven triboelectric nanogenerator for wind energy harvesting and application in smart agriculture, *Appl. Energy* 306 (2022), 117977.
- [48] L. Long, W.L. Liu, Z. Wang, W.C. He, G. Li, Q. Tang, H.Y. Guo, X.J. Pu, Y.K. Liu, C. G. Hu, High performance floating self-excited sliding triboelectric nanogenerator for micro mechanical energy harvesting, *Nat. Commun.* 12 (2021) 4689.



Yuqi Wang was born in 1995 Jilin province, majored in mechatronic engineering and achieved the B.E. degree from the Changchun University of Technology in 2018. He continues pursuing a Master of Engineering degree in the same school. He is currently a visiting student at Beijing Institute of Nanoenergy and Nanosystems. His research interests are environmental energy harvesting through triboelectric nanogenerators.



Xiang Li achieved the B.S. degree from the Shenyang University of Technology in 2018. He is studying for a master's (M.S.) degree in mechanical engineering at Shenyang Jianzhu University. Now, he is a visiting student at Beijing Institute of Nanoenergy and Nanosystems. His research interest is environmental energy harvesting by triboelectric nanogenerators.



Dr. Xin Yu is a visiting scholar in Beijing Institute of Nanoenergy and Nanosystems, Chinese Academy of Sciences, currently. He obtained the B.S. and Ph.D. degrees from College of Electronic Science and Engineering, Jilin University in 2009 and 2014, respectively. He was a visiting scholar in Department of Electrical and Computer Engineering, Michigan State University from 2017 to 2018. His interests are triboelectric nanogenerators, infrared gas sensing, and photoelectric detection.



Dr. Jianyang Zhu received his B.S. and M.S. from Harbin Institute of Technology University, China in 2006 and 2008, respectively, and his Ph.D. in Fluid Machinery and Engineering in 2014. He is currently an assistant professor of Machinery and Automation at Wuhan University of Science and Technology in Wuhan, China. His research interests include fluid-structure interaction, fluid dynamics, and heat transfer.



Dr. Ping Shen received his Ph.D. from the Hong Kong University of Science and Technology in 2019. Nowadays, he is an assistant professor in State Key Laboratory of Internet of Things for Smart City and Department of Civil and Environmental Engineering, University of Macau. His research interests mainly include rain-induced multi-hazard simulation, coastal urban hazard analysis, hazard monitoring and mitigation and risk assessment and management.



Prof. Zhong Lin Wang received his Ph.D. from Arizona State University in physics. He now is the Hightower Chair in Materials Science and Engineering, Regents' Professor, Engineering Distinguished Professor and Director, Center for Nanostructure Characterization, at Georgia Tech. Dr. Wang has made original and innovative contributions to the synthesis, discovery, characterization and understanding of fundamental physical properties of oxide nanobelts and nanowires, as well as applications of nanowires in energy sciences, electronics, optoelectronics and biological science. His discovery and breakthroughs in developing nanogenerators established the principle and technological road map for harvesting mechanical energy from environment and biological systems for powering personal electronics. His research on self-powered nanosystems has inspired the worldwide effort in academia and industry for studying energy for micro-nano-systems, which is now a distinct disciplinary in energy research and future sensor networks. He coined and pioneered the field of piezotronics and piezophotonics by introducing piezoelectric potential gated charge transport process in fabricating new electronic and optoelectronic devices. Details can be found at: [http:// www.nanoscience.gatech.edu](http://www.nanoscience.gatech.edu).



Prof. Tinghai Cheng received the B.S., M.S. and Ph.D. degrees from Harbin Institute of Technology in 2006, 2008 and 2013, respectively. He was a visiting scholar in the School of Materials Science and Engineering at Georgia Institute of Technology from 2017 to 2018. Currently, he is a professor of Beijing Institute of Nanoenergy and Nanosystems, Chinese Academy of Sciences. His research interests are triboelectric nanogenerators, piezoelectric energy harvester, and piezoelectric actuators.